Paper

Development of Si/SiO$_2$ Multilayer Type AFM Tip Characterizers

Hisataka Takenaka,[1]* Masatoshi Hatayama,[1] Hisashi Ito,[1] Tadayuki Ohchi,[1] Akio Takano,[1]

Satoru Kurosawa, [1] Hiroshi Itoh[2] and Shingo Ichimura[2]

[1]*NTT Advanced Technology Co., 3-1 Morinosato Wakamiya, Atsugi, Kanagawa, 243-0124, Japan*

[2]*National Institute of Advanced Industrial Science and Technology, Tsukuba Central 2, 1-1-1 Umezono, Tsukuba, Ibaraki, 305-8568, Japan*

*hisataka.takenaka@ntt-at.co.jp

A new type of AFM tip characterizer used for characterizing nanostructures in the 10 nm to 100 nm range was developed. The characterizer was fabricated by preferential etching the edge of a cross sectioned Si/SiO$_2$ multilayer. Both isolated line structures and line-and-space structures were fabricated. The structural and practical properties of the fabricated tip characterizer were evaluated, and it was shown that it can be used to characterize AFM tip shapes in the 10 nm to 100 nm range.

1. Introduction

In recent years, tip characterizers for atomic force microscopy (AFM) with measurement ranges from 10 nm to 100 nm have been sought after by AFM tip vendors and AFM users alike. There are two reasons for this; (i) the tip radius of a conventional AFM tip is typically 10 nm, (ii) the development of nanofabrication techniques such as electron-beam lithography, nanoimprinting, and etching techniques has enabled high-aspect ratio 10 nm width features to be fabricated. Several algorithms to reconstruct the shape of AFM tips have been reported [1-3]. At the same time, tip characterizers have also been reported. Spherical structures such as colloidal gold [4], polystyrene or glass spheres [5, 6], nanofabricated spheres [7], hole grid patterns [8], quantum dots [9], dot grid patterns [10], needle-shaped samples [11] and other nanostructures [12] have been demonstrated. However, it is difficult to evaluate the fine shape of an AFM tip, especially that of the sides. To address this issue, a characterizer with line-and-space (L&S) patterns fabricated using electron beam lithography was demonstrated [13]. However, this was limited to pattern-widths of not less than 20 nm. Furthermore, with this method it was difficult to make high aspect ratio structures. Recently, a new tip characterizer with a 10-nm wide structure was developed using GaAs/InGaP superlattices [14]. L&S patterns in the 10 nm range and high aspect ratios were realized with this superlattice type characterizer. However, this
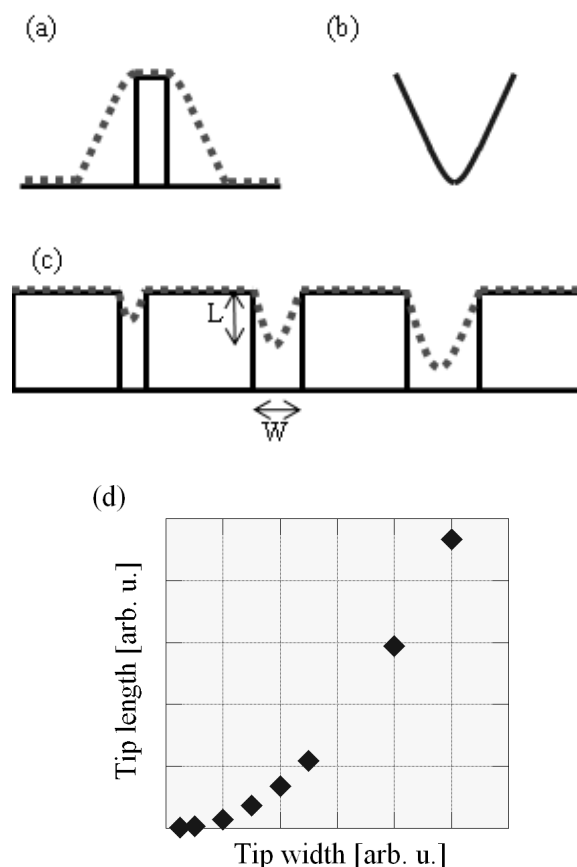

Fig. 1 Schematics of the AFM tip characterization. (a) AFM profile of an isolated line structure and (b) the reconstructed tip shape. (c) AFM profile of L&S structures and (d) the reconstructed relationship between the tip width and length.

characterizer cannot be used in the bio-medical and Si nanodevice fields because GaAs is toxic and a source of contamination, respectively.

In this paper, we developed a Si/SiO$_2$ multilayer type tip characterizer which included several step nanostructures. This characterizer was designed with 10 nm and 20 nm isolated line patterns and L&S structures with trenches ranging from 7.5 nm to 130 nm in width. Furthermore, we demonstrated the characterization of a pyramidal type Si AFM tip shape in the around 10 nm to 100 nm range using the tip characterizer.

2. Design and Fabrication

The AFM tip characterizer was designed for characterizing AFM tips in the 7.5 nm to 100 nm range. Isolated line structures with line widths of 10 nm and 20 nm were included in the characterizer. AFM images of these structures show the inverse tip surface as shown in Fig. 1(a) and Fig. 1(b) [11]. Twelve step L&S structures with trench widths ranging from 7.5 nm to 130 nm were also included in the characterizer as shown in Fig. 1(c). From each fabricated trench width and measured depth of the AFM image (labeled "W" and "L" in Fig. 1(c), respectively), the relationship between the tip width (the trench width of the L&S structure) and the tip length (the measured depth obtained from trajectory of tip apex, as is shown schematically in Fig. 1(c)) was obtained as shown in Fig. 1(d) [15].

The fabrication procedure of the Si/SiO$_2$ multilayer type tip characterizer is shown in Fig. 2. In the first step, a Si/SiO$_2$ multilayer was deposited on Si wafers as shown in Fig. 2(a) using magnetron sputtering. With this system, schematically shown in Fig. 3, the thickness of each layer of material can be controlled to better than 3%. Secondly, two pieces of wafer were bonded using the surface activated room temperature wafer bonding method [16] with the multilayered surfaces facing each other (Fig. 2(b)). In the third step, the bonded wafers were cut into pieces perpendicular to the surface (Fig. 2(c)). Fourthly, each piece was mounted on a Si base plate and the cross-sectional plane was chemical mechanically polished (Fig. 2(d)). Finally the SiO$_2$ layers were selectively etched in a HF solution (Fig. 2(e)) and Si isolated line structures and Si/SiO$_2$ L&S structures were developed.

This Si/SiO$_2$ type tip characterizer has several advantages compared with GaAs/InGaP superlattice type tip characterizers. First, the materials from which the tips are constructed are highly compatible with Si nanodevices such as
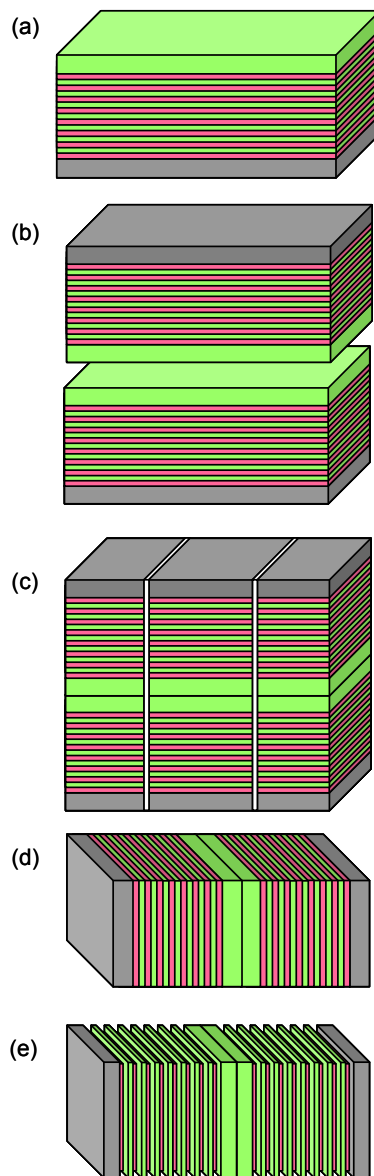

Fig. 2 Fabrication procedure for the Si/SiO$_2$ multilayer type AFM tip characterizer. (a) Si/SiO$_2$ multilayer deposition process, (b) wafer bonding process, (c) wafer cutting process, (d) cross-sectional plane polishing process, and (e) chemical etching process.
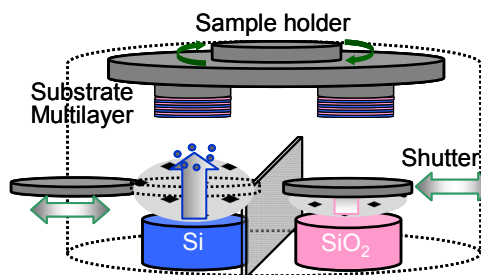

Fig. 3 Si/SiO$_2$ sputtering system.

Journal of Surface Analysis Vol.17, No.3 (2011) pp.264-268

H. Takenaka et. al.   Development of Si/SiO2 Multilayer Type AFM Tip Characterizers.
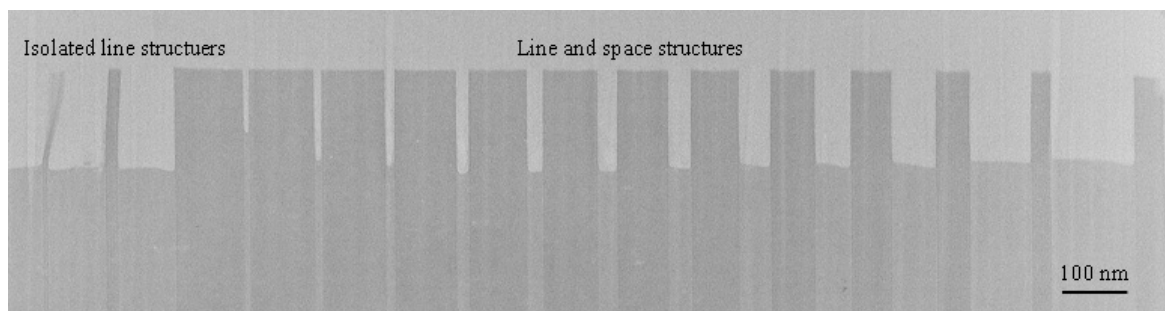
Fig. 4 Cross-sectional TEM image of fabricated Si/SiO2 tip characterizer.

LSI. Secondly, HF solution can easily etch narrow high aspect ratio structures, whereas the high viscosity of H_2SO_4 solution, used for selectively etching GaAs, makes it more difficult to achieve the same high aspect ratios. Thus, the tip characterizer fabricated in this work can be made with higher aspect ratios. A third advantage of the Si/SiO2 tip characterizer is that it is biologically non-toxic and can be used safely.

3. Evaluations

A cross-sectional transmission electron microscope (TEM) image of the fabricated tip characterizer is shown in Fig. 4. The obtained isolated line widths are 10.0 nm and 20.1 nm, and the obtained trench widths of the L&S structures range from 7.7 nm to 131 nm. These widths are 1–3% greater than the designed values. This is believed to be due to fluctuations in the deposition rate causing the pattern widths to increase.

The cross-sectional TEM image shows that the surface of the tip characterizer is not perpendicular to the Si/SiO2 interfaces. This tilt, which is less than 0.5 degrees, is thought to be not significant, because the variation in the aperture of each trench due to this is estimated to be less than 1%. Note that the 10 nm wide isolated lines have become distorted for etch depths greater than 80 nm. The stiffness depends on the aspect ratio and the limitation for the line structure is an aspect ratio of 8. On the other hand, the limiting aspect ratio for the space pattern is 13.

To evaluate the practical properties of the tip characterizer, AFM images of it were measured across the trenches using a pyramidal Si tip in the intermittent contact mode. The tip specification is shown in Table 1. An AFM image of isolated line structures scanned in the direction of the lines is shown in Fig. 5. To reconstruct the tip shape, the measured profile was inverted in the x– and y–directions and then, the line width of the characterizer was subtracted from the profile. The tip shapes reconstructed from the 10 nm (circles)

and 20 nm isolated line structures (diamonds) are shown in Fig. 6. The results show that the apex diameter and half cone angle of the AFM tip are estimated to be 9 nm and 19°, respectively. On the other hand, an AFM image obtained for L&S structures scanned parallel to the patterns is shown in Fig. 7 and the tip width-depth curve obtained from this image is shown in Fig. 8. The half cone angle of the tip is estimated to be 21°. The estimated apex diameter shows good agreement with the specification. However, the half cone angle was over estimated. These results show that the reconstructed tip shape depends on the installation and measurement conditions. This kind of *in situ* tip information cannot be obtained from typical specification notes.

Table 1 Specification of a standard Si AFM tip.

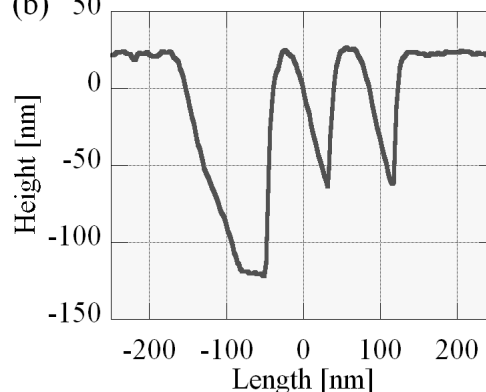|	
apex diameter	<10 nm
half cone angle	10 °

(a)

(b)

Fig. 5 (a) Obtained AFM image of isolated line structures and (b) cross-sectional image. Each line width is either 10 nm or 20 nm.

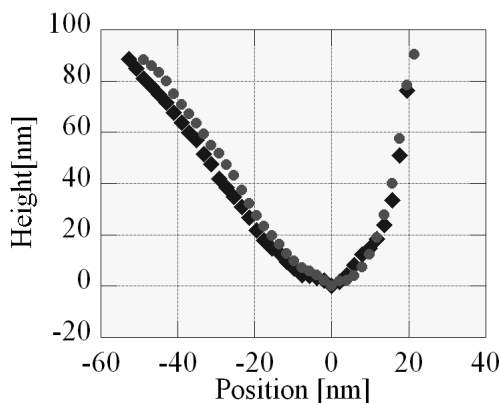*Journal of Surface Analysis Vol.17, No.3 (2011) pp.264-268*

H. Takenaka et. al.   Development of Si/SiO$_2$ Multilayer Type AFM Tip Characterizers.

Fig. 6 Characterized AFM tip profiles using 10 nm (circles) and 20 nm isolated lines (diamonds).
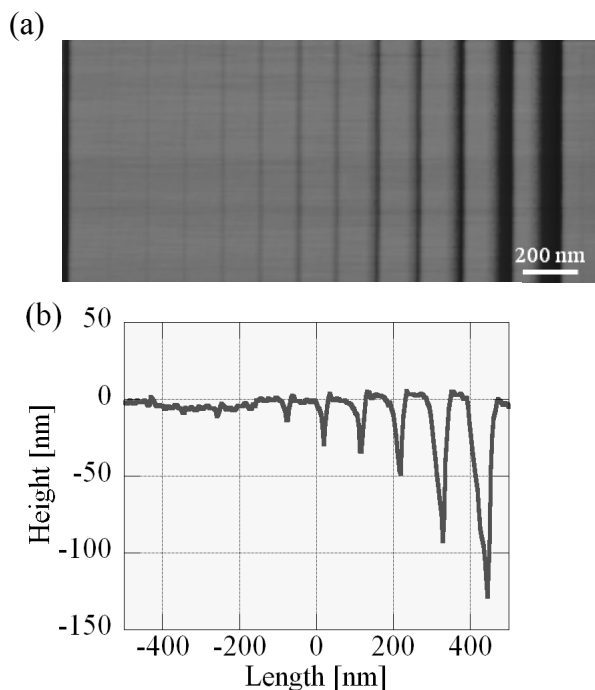
(a)

(b)

Fig. 7 (a) Obtained AFM image of the L&S structures and (b) cross-sectional profile.

4. Conclusions

A Si/SiO$_2$ multilayer type AFM tip characterizer having isolated line structures and L&S structures with widths ranging from 5 nm to 100 nm was developed and evaluated using cross-sectional TEM. The measured isolated line structure widths were 10.0 nm and 20.1 nm, and the measured trench widths of the L&S structures ranged from 7.7 nm to 131 nm, which are in good agreement with the designed values. The isolated line-and-space patterns had aspect ratios of up to 8 and 13, respectively.

The shape of a pyramid type Si AFM tip was

reconstructed using the fabricated tip characterizer. The results show that this characterizer can be used to characterize AFM tip shapes ranging from 10 nm to 100 nm.
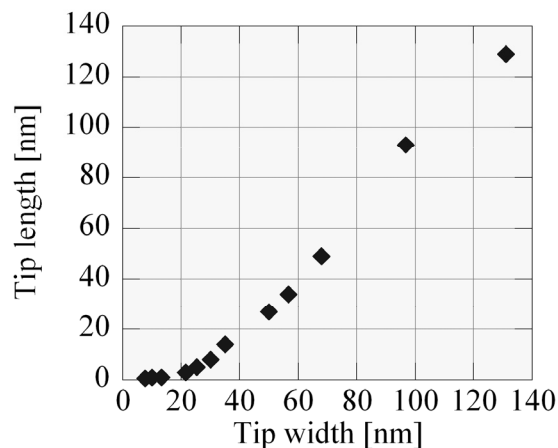

Fig. 8 Reconstructed tip width and length from L&S structure measurements.

References

[1] R. Dixson, N. Sullivan, J. Schneirl, T. McWaidl, V. W. Tsai, J. Prochazka and M. Young, *Proc. SPIE* **2725**, 572 (1996).

[2] J. S. Villarrubia, *J. Res. Natl. Inst. Stand. Technol.* **102**, 425 (1997).

[3] L. S. Dongmo, J. S. Villarrubia, S. N. Jones, T. B. Renegar, M. T. Postek and J. F. Song, *Ultramicroscopy* **85**, 141 (2000).

[4] S. Xu and M. F. Arnsdorf, *J. Microsopy* **173**, 199 (1994).

[5] Y. Liand and S. M. Lindsay, *Rev. Sci. Instrum.* **62**, 2630 (1991).

[6] K. A. R.-Aguilar and K. L. Rowlen, *Langmuir* **14**, 2562 (1998).

[7] K. L. Westra, A. W. Mitchell and D. J. Thomson, *J. Appl. Phys.* **74**, 3608 (1993).

[8] P. Markiewicz and M. C. Goh, *Rev. Sci. Instrum.* **66**, 3186 (1995).

[9] K. Shiramine, S. Muto, T. Shibayama, N. Sakaguchi, H. Ichinose, T. Kozaki, S. Sato, Y. Nakata, N. Yokoyama and M. Taniwaki, *J. Appl. Phys.* **101**, 033527 (2007).

[10] Y. Harada, H. Sone and S. Hosaka, *Jpn. J. Appl. Phys.* **47**, 6186 (2008).

[11] D. Fujia, H. Itoh, S. Ichimura and T. Kurosawa, *Nanotechnology* **18**, 084002 (2007).

[12] V. Bykov, A. Gologanov and V. Shevyakov, *Appl. Phys.* **A 66**, 499 (1998).

[13] M. Nagase, H. Namatsu, K. Kurihara, K. Iwadate and K. Murase, *Jpn. J. Appl. Phys.* **34**, 3382 (1995).

[14] H. Itoh, T. Fujimoto and S. Ichimura, *Rev. Sci. Instrum.* **77**,103704 (2006).

[15] M. Xu, D. Fujita and K. Onishi, *Rev. Sci. Instrum.* **80**, 043703 (2009).

[16] H. Takagi, K. Kikuchi, R. Maeda, T. R. Chang and T. Suga, *Appl. Phys. Lett.* **68**, 2222 (1996).